Transaction B: Mechanical Engineering
Vol. 17, No. 5, pp. 358–366

SCIENTIA IRANICA

Investigation of Wall Shear Stress Related Factors in Realistic Carotid Bifurcation Geometries and Different Flow Conditions

S.S. Jamalian Ardakani[1], M. Jafarnejad[1], B. Firoozabadi[1,*] and M.S. Saidi[1]

Abstract. *Cardiovascular diseases are one of the major causes of death in the world; atherosclerosis being one aspect. Carotid bifurcation is one of the sites that are vulnerable to this disease. Wall Shear Stress (WSS) is known to be responsible for the process of atherogenesis. In this study, we have simulated the blood flow for Newtonian and non-Newtonian, steady and unsteady, flow conditions in three idealistic and five realistic geometries. A risk factor has been presented based on the results of wall shear stress and, then, a relation was found between geometrical features and the wall shear stress risk factor. Our main conclusions are: 1) The non-Newtonian behavior of blood elevates the value of wall shear stress, however, the wall shear stress pattern is similar, 2) The bifurcation angle is not the main cause of atherosclerosis and cannot be considered a predictor for atherosclerosis disease, and 3) The ratio of sinus diameter to the internal carotid artery diameter is more important than other geometrical factors, and the WSS pattern is influenced by this factor.*

Keywords: *Carotid bifurcation; Wall shear stress; Geometry effect; Non-Newtonian; Bifurcation angle; Sinus diameter.*

INTRODUCTION

One major cause of human death in the world is cardiovascular disease [1]. Atherosclerosis is more likely to occur at special blood vessels. According to medical data, carotid artery bifurcation is one of the vessels that are vulnerable to atherosclerosis. Previous studies have proved that shear stress on the vessel wall is an important factor in atherogenesis [1]. Based on previous investigations, we know that atherosclerosis usually occurs at sites of the vessel wall with low average shear stress or highly oscillatory shear stress [2,3]. It is also known that the complicated geometry of the carotid bifurcation can affect the blood flow pattern [4-6]. As a result, the magnitude and pattern of wall shear stress in carotid bifurcation depends on the unique geometry of the vessel. The bifurcation angle can be considered an important geometry factor [7,8] which can affect the flow pattern in the sinus of an Internal Carotid Artery (ICA), the most atheroprone site in bifurcation [4]. In this study, we investigated the effects of two of the carotid bifurcation geometrical parameters on the wall shear stress pattern. These parameters are the bifurcation angle and the sinus bulb diameter. According to Goubergrits et al. [9], the bifurcation angle is related to gender. Based on their experimental studies, the bifurcation angle in men is larger than women. The average female bifurcation angle is 51 degrees and the average male bifurcation angle is 67 degrees [9]. In order to determine the effect of bifurcation angle, we have developed three models of carotid bifurcation with different bifurcation angles; one representing a female carotid, one a male carotid, and one somewhere in between. This angle may possibly occur in both genders. Then, we examined the effect of bifurcation angle on the wall shear stress. Several investigators have simulated blood flow in carotid bifurcation, experimentally [10-14]. They have constructed an experimental model of the bifurcation and investigated the flow within. Their geometries were an ideal geometry as a representation of carotid bifurcation, but they have not obtained their geometry from real carotid bifurcation geometry. Studies have

1. *School of Mechanical Engineering, Sharif University of Technology, Tehran, P.O. Box 11155-9567, Iran.*
*. *Corresponding author. E-mail: firoozabadi@sharif.edu*

Received 3 December 2009; received in revised form 6 June 2010; accepted 3 July 2010

shown that carotid bifurcation geometry differs from person to person [9,15-17]. Researchers, considering the effect of geometry on the flow pattern and its relation to cardiovascular disease, reconstructed their simulation models from patient specific data [4,5,18-20]. In order to make sure that the bifurcation angle effect we have observed is also true in realistic geometry, we have investigated five realistic geometries reconstructed from patient specific data.

We have compared our CFD results with distribution of the atherosclerotic lesions provided by pathomorphometrical analysis by Goubergrits et al. [9]. Apart from the vessel itself, we must also consider the flow within. The blood that is flowing inside our vessels is a non-Newtonian fluid. Some investigators suggested that in large blood vessels like carotid bifurcation, the blood can be assumed as Newtonian fluid [5,21]. However, some others preferred to model blood with non-Newtonian models [13,22,23]. We have also investigated the effects of non-Newtonian blood models on ideal carotids with different bifurcation angles. Several investigators have modeled the steady blood flow in carotid bifurcation [10,13] while others preferred to model the blood flow as unsteady, which is more realistic [5,20,21,24-27]. In the present study, the unsteady blood flow has also been solved in three realistic geometries, in order to study the WSS under unsteady flow conditions.

METHOD

In this work, we examine eight geometries (presented in Figures 1 and 2), three of which are constructed according to realistic dimensions and shapes. Our ideal geometry is a 3D reconstruction of Bhardavaj et al.'s experimental model [28,29] (Figure 1b). Bhardvaj et al. presented a 2D model of carotid bifurcation geometry with realistic scales, which we used to construct the 3D geometry. The other two geometries have the same general shape, but with different angles. These

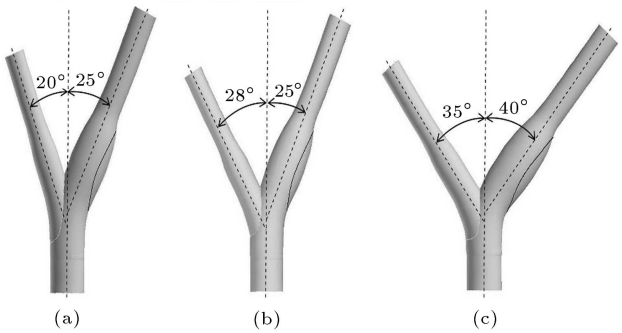

Figure 1. Three ideal carotid bifurcation geometries. (a) Sample model for female carotid bifurcation. (b) Ideal geometry of Bhardvaj et al. [28,29]. (c) Sample model for male carotid bifurcation.

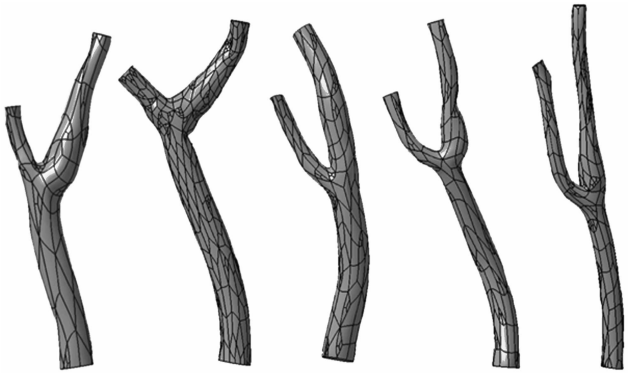

Figure 2. Five realistic carotid bifurcation geometries.

two different angles were chosen as a representation of female and male carotid bifurcations (Figures 1a and 1c, respectively, and Table 1) [9]. The other five geometries are reconstructed from patient specific data (Figure 2, Table 2). The vessel casts were carved arteries. The blood vessels were filled by a filler substance. Using the morphometrical analysis of Goubergrits et al. [9], we imposed optimized mean surfaces from the available points and reconstructed our geometries (Figure 2).

According to our assumptions presented earlier, Navier-Stokes Equation 1 and continuity Equation 2 for the incompressible and isothermal flow of a Newtonian fluid are solved in a 3D geometry. These equations are listed below:

$$\rho\frac{\partial u}{\partial t} + \rho(u.\nabla)u = -\nabla P + \rho g + \mu\nabla^2 u, \quad (1)$$

$$\nabla.u = 0. \quad (2)$$

In these equations, ρ represents density, u represents velocity, P is pressure, g is gravity constant and θ the viscosity.

In this work, the finite volume method has been applied to obtain a numerical solution for blood flow simulations with segregated 3D solver. The computational tetrahedral grids were generated as shown in

Table 1. Geometrical features of ideal geometries.

Case Number	1	2	3
Diameter of CCA (mm)	8.00	8.00	8.00
Diameter of ECA (mm)	4.60	4.60	4.60
Diameter of Sinus (mm)	8.90	8.90	8.90
Diameter of ICA (mm)	5.60	5.60	5.60
Branch Angle Between CCA and ICA (degree)	25	25	40
Branch Angle Between CCA and ECA (degree)	28	20	35

Table 2. Geometrical features of all realistic cases.

Case Number	4	5	6	7	8
Age	82	80	90	81	–
Sex	Female	Male	Female	Male	–
Side	Right	Right	Left	Left	Left
Basic Disease of Death	Atherosclerotic disease	EPOC	Hypertension disease	Atherosclerotic disease	–
Direct Cause of Death	Sepsis	Bronchopneumonia	Encefalopatia Hipertensiva	IMA	–
Diameter of CCA (mm)	7.25	7.60	6.80	7.48	5.7
Diameter of ECA (mm)	5.10	5.60	4.35	5.35	4.6
Diameter of Sinus (mm)	8.55	8.68	6.60	8.00	7.4
Diameter of ICA (mm)	6.22	6.25	6.45	5.70	4.9
Branch Angle Between CCA and ICA (degree)	27	44	9	45	34
Branch Angle Between CCA and ECA (degree)	13	31	20	42	50

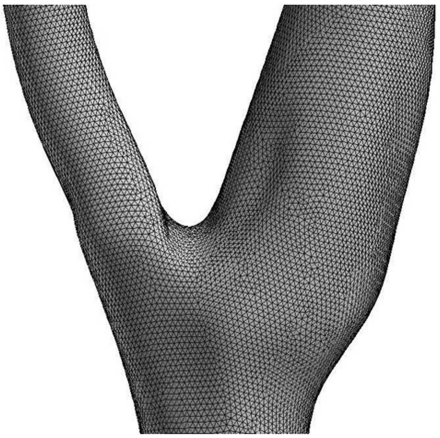

Figure 3. A sample representation of a generated computational grid for geometry of case 4 shown in Table 2.

Figure 3. The grid independency was checked for one of the geometries as a sample. The average grid element was 0.25 mm and the pressure-velocity coupling is handled by the SIMPLEC method. The convective terms are treated by the hybrid scheme. TDMA-based algorithms are applied for solving the algebraic equations. The solution procedure is iterative and the computations are terminated when the sums of absolute residuals normalized by the inflow fluxes are below 10^{-4} for all variables. For the ideal geometries boundary condition, we applied the parabolic velocity profile for the Common Carotid Artery (CCA) inlet; this results in a Re number (based on carotid diameter) equal to 300. Here, a steady mass flow rate has been used for a CAA inflow boundary condition. This mass flow rate has been set in order to keep the inlet Re number the same in all cases. Constant realistic values for Re, μ, ρ and d were set and, then, the average velocity was calculated. According to these calculations, the mass flow rate would change for different geometries. These values are presented in Table 3.

On the carotid walls, no-slip boundary conditions were set due to viscosity effects. The outflow boundary condition was set for an Internal Carotid Artery (ICA) and an External Carotid Artery (ECA). The division of the flow into ICA and ECA was assumed to be proportional to their cubic diameters. Wootton et al. [12] reported a mean Reynolds number of around 300 for blood flow in the carotid artery. Gijsen et al. [13] have set Re = 270 as the inflow Re number; we have assumed this value for the Re number for average velocity calculations. In order to check the validity of these assumptions, the flow rates were compared with the measurements of Marshall et al. [26], and presented a good agreement. The flow rates for the common, external and internal carotids and the results of Marshall et al. [26] are shown in Table 3.

The steady flow was solved for both Newtonian and non-Newtonian blood flow models in all eight geometries. In the present study, blood is once assumed to be a Newtonian fluid with a density of 1060 kg/m^3 and a dynamic viscosity of 0.00345 kg/(m.s). The mass flow rate has been calculated in CCA, ICA and ECA. Mass flow rate values have been compared to the experimental data of Marshal et al. [26] to make sure that they are in the accepted interval for the carotid mass flow rate. The non-Newtonian behavior of blood

Table 3. Verification of blood flow rate in all geometries with the results of Marshal et al. [26].

Geometry	Reynolds Number	CCA Mass Flow Rate (kg/s)	ICA Mass Flow Rate (kg/s)	ECA Mass Flow Rate (kg/s)
Three idealistic	270	0.00585	0.00322	0.00263
4	270	0.00529	0.00380	0.00209
5	270	0.00556	0.00323	0.00233
6	270	0.00497	0.00380	0.00117
7	270	0.00546	0.00299	0.00247
8	270	0.00417	0.00228	0.00189
Marshal et al. [26]		0.00646	0.00434	0.00166

is modeled by Carreau whose model constants have been set with reference to the work of Jahanifard et al. [23].

$$\mu = \mu_\infty + (\mu_0 - \mu_\infty)[1 + (\lambda\dot{\gamma})^2]^{(n-1)/2}, \quad (3)$$

where:

$\lambda = 3.313$,
$n = 0.3568$,
$\mu_0 = 0.056$ Pa.s,
$\mu_\infty = 0.00345$ Pa.s,
$\dot{\gamma} =$ Strain rate.

Our main focus of study was investigation of the Wall Shear Stress (WSS) in different carotid bifurcation geometries of Newtonian and non Newtonian steady blood flow. It is well known that the blood flow in carotid bifurcation is unsteady. In order to understand the unsteady nature of blood flow, we have solved the unsteady solution for geometries 1, 2 and 3. Here, a typical carotid bifurcation pulse was set for the inlet boundary condition and the outlet boundaries were set to be stress free outflow. Based on the unsteady solution, we compared the WSS pulse in the carotid bifurcation and the sinus region.

RESULTS AND DISCUSSION

The Newtonian and non-Newtonian blood flow has been solved in all eight geometries. To validate our solution, we have compared our results for case 1 (shown in Table 1) [28,29] with the experimental results of Gijsen et al. [13]. They had used this sample geometry for their experimental setup. Figure 4 shows the comparison between our numerical results and Gijsen et al. [13] experimental results for the Newtonian case. According to this comparison, our numerical results follow the experiments very well. However, small differences exist; numerical inaccuracy causing the differences between our results and the experiment. By using a structured instead of tetrahedral grid, the results could be improved. Apart from this, Gijsen et al. [13] used a substance as a representation of blood in their model that had minor differences in viscosity and behavior with real blood. However, the differences, in general, are negligible.

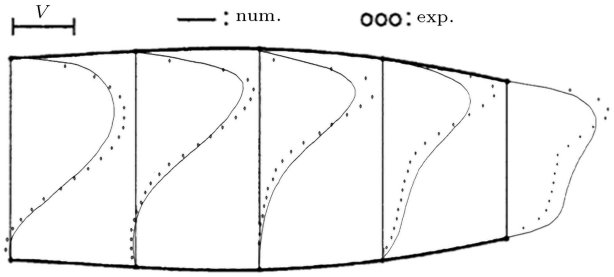

Figure 4. Comparison between experimental results of Gijsen et al. [13] and our CFD results for geometry case 1 (shown in Table 1). In this picture, the internal carotid bifurcation has been presented. Velocity profiles have been plotted in five sections through the ICA. The velocity unit shown is equal to 0.07 m/s.

It is known that the wall shear stress is an important factor in progression and initiation of atherosclerosis [1,2]. Figure 5 shows the WSS contour for case 1, shown in Table 1, and all realistic geometries (cases 4-8 shown in Table 2). According to Malek et al. [2], regions with WSS less than 0.4 Pa are susceptible to atherosclerosis [2]. Here, in wall shear stress contours, we have separated the regions with shear stress below 0.4 Pa, in order to separate atheroprone sites, which are represented in dark blue.

A general conclusion from these WSS patterns is that the sinus bulb is the most atheroprone site where higher values of WSS appear at the bifurcation apex and final ends of the External Carotid Artery (ECA) and ICA, which have a lower diameter. There is a stagnation point at the apex because the shear directions at its sides are different (although the magnitude of the shear would be high). According to Goubergrits et al. [9], the stagnation point is the place of plaque buildup. Another point is that, in general, realistic geometries have higher values of WSS and the atheroprone site in the sinus bulb is smaller

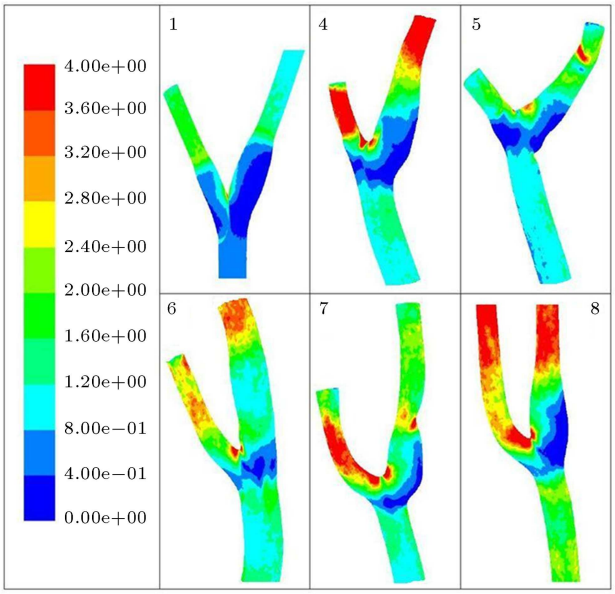

Figure 5. WSS contours for case 1 and all realistic cases. The regions represented in dark blue show the atheroprone sites.

in these geometries. Therefore, the complexity of the realistic geometry is an atheroprotective factor, because it results in higher values of shear stress.

To show the difference in WSS in different geometries, we have calculated the average WSS and sinus average WSS for all cases. Table 4 presents the WSS values for Newtonian and non-Newtonian blood models. The non-Newtonian model elevates the average WSS and sinus average WSS in all cases, so the non-Newtonian behavior of blood is an atheroprotective behavior. Soulis et al. [22] studied the non-Newtonian behavior of blood in the left coronary artery. They have found the non-Newtonian behavior to be atheroprotective as well. The non-Newtonian effect can elevate critical WSS in such a way that it is no longer critical. So, the critical value of WSS should be modified considering Newtonian or non-Newtonian blood. In order to quantify the non-Newtonian effects, we have introduced a Non-Newtonian Effect Factor (NNEF), which shows the percent difference between the Newtonian and non-Newtonian solution.

$$\text{NNEF} = \frac{(\text{non Newtonian})_{\text{WSS}} - (\text{Newtonian})_{\text{WSS}}}{(\text{Newtonian})_{\text{WSS}}} \times 100. \quad (4)$$

Although the NNEF is different for each case, the arithmetic average of the NNEF factor for ideal geometry is 14%, while it is about 10% for realistic geometries, which means that the non-Newtonian effect is lower in realistic cases. The average NNEF for a critical wall shear zone in a sinus bulb is 18% and 50% for realistic and ideal cases, respectively. So, the non-Newtonian effect is not the same over different sites of carotid bifurcation. As an example, the non-Newtonian effect in a carotid sinus is distinguishably more than the whole geometry of carotid bifurcation. The calculated NNEF for each case is presented in Table 4.

We have also solved the unsteady case for our three idealistic geometries. Figure 6 shows the total WSS and sinus WSS during one pulse. The results for the other two ideal cases were the same with a slight change in magnitude. Here, again, sinus WSS is much lower than total WSS and has low fluctuations in comparison with the total shear wave.

In their study of WSS in carotid bifurcation, Mofrad et al. [20] reported that a high cyclic stretch is responsible for atherosclerosis. Based on this hypothesis, they could not explain why atherosclerosis lesions occur at the sinus bulb. According to Figure 6, it can be concluded that what makes the sinus bulb of the

Table 4. Average values of WSS and Sinus WSS for Newtonian and non-Newtonian blood models in all cases. The NNEF percent shows the effect of non-Newtonian models for each case.

Geometry	Average Sinus WSS Newtonian (Pa)	Average Sinus WSS Non-Newtonian (Pa)	NNEF Sinus (%)	Average Net WSS Newtonian (Pa)	Average Net WSS Non-Newtonian (Pa)	NNEF Net (%)
1 (58°)	0.0855	1.0054	57.4	1.0054	1.1526	14.6
2 (45°)	0.1065	1.0112	50.6	1.0112	1.1562	14.3
3 (75°)	0.1276	1.0216	47.2	1.0216	1.1627	13.8
4 (40°)	0.3797	1.8059	17.2	1.8059	1.9761	9.4
5 (75°)	0.4411	1.2208	21.5	1.2208	1.3753	12.7
6 (29°)	0.9225	1.6633	18.1	1.6633	1.8607	11.9
7 (87°)	0.3568	1.5697	14.4	1.5697	1.7410	10.9
8 (84°)	0.3436	2.4627	18.4	2.4627	2.6363	7.1

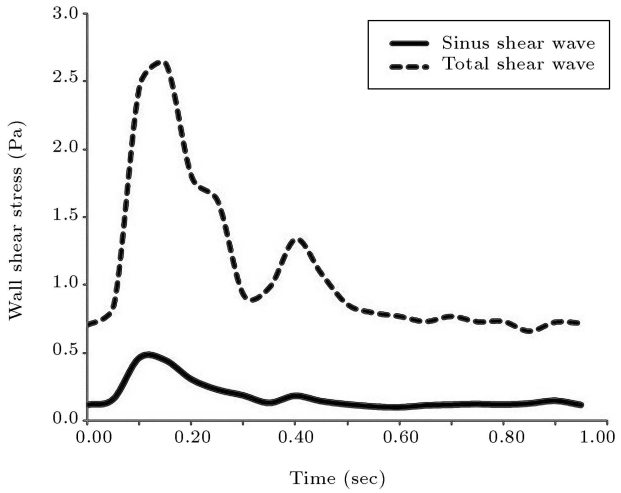

Figure 6. Total shear wave and sinus shear wave for unsteady solution of geometry case 1 (Table 1) during one heartbeat.

carotid bifurcation an atheroprone site is its very low WSS magnitude and not its highly oscillatory shear wave. We have also introduced an atherosclerosis risk factor for carotid bifurcation. This factor is the area percentage of carotid bifurcation that experiences a WSS magnitude less than 0.4 Pa. Figure 7 represents this risk factor for Newtonian and non-Newtonian blood models in eight geometries. Here, again, there is a difference between ideal and realistic geometries and, as we expected from previous results, the non-Newtonian risk is lower than the Newtonian risk.

Several investigators have presented geometrical factors like bifurcation angle, off plane angle or sinus diameter, as geometrical risk factors [7,6,19]. We have also investigated the relation between geometrical features of carotid bifurcation and WSS. Our three ideal geometries (cases 1 to 3 shown in Table 1) have the same diameters of inlet and outlet and the same geometrical features (the curvature and sinus diameters).

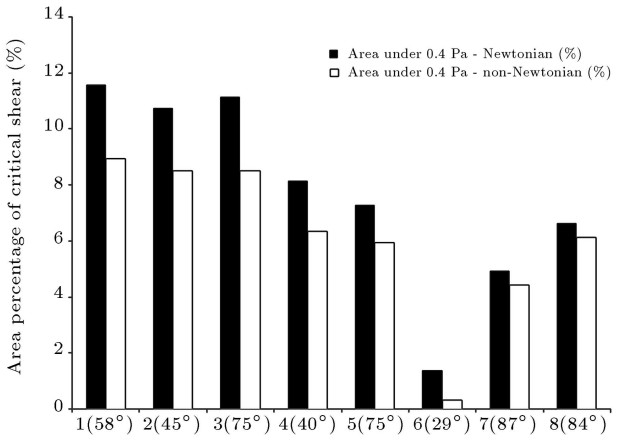

Figure 7. The area percent with WSS < 0.4 Pa for Newtonian and non-Newtonian cases.

The only difference between them is the bifurcation angle. A comparison between these cases and their WSS shows that a lower bifurcation angle results in a lower average WSS and a lower average sinus WSS. However, this result is not valid for realistic bifurcations. So, prediction of the carotid bifurcation atherosclerosis risk factor based on idealistic geometries cannot be used as a confident prediction in realistic geometries. These findings seriously challenge the results of previous investigators who have made such a prediction [7,9]. These studies have only investigated ideal geometries and introduced risk factors based on these results; which our study proves inconvenient. We have also investigated the relationship between $D_{\text{sinus}}/D_{\text{ICA}}$ and the atherosclerosis risk factor. Figure 8 represents the atherosclerosis risk factor, which is the area with WSS lower than 0.4 Pa, $D_{\text{sinus}}/D_{\text{ICA}}$ and bifurcation angle for each geometry case. According to this graph, the trend of the magnitudes of atherosclerosis risk factor is the same as $D_{\text{sinus}}/D_{\text{ICA}}$. However, no satisfactory relation can be found between bifurcation angle or sinus diameter itself and atherosclerosis risk factor.

The pathomorphometrical results are compared with the WSS contours in order to find a relation between diseased sites and the magnitude of WSS. The results of pathomorphometrical analysis show the distribution and alteration level of the atherosclerotic lesions in carotid bifurcations. Figure 9 provides a comparison between the WSS results of our CFD solution and the pathomorphometrical analysis for geometry cases 4, 5, 6 and 7. The blue marks show fatty streaks and the red one fibrous plaque. The fibrous plaques are exactly coagulated at the site of low shear stress. In sites with higher WSS, there are only sporadic fatty streaks, which are not considered as a risk factor.

It can be concluded that fatty streaks and fibrous plaques are only life threatening if they are agglom-

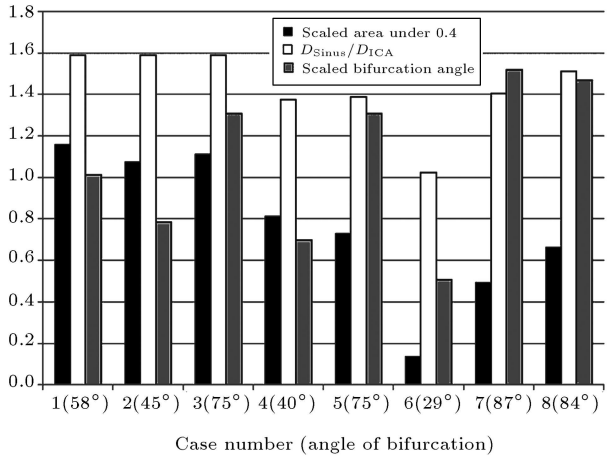

Figure 8. The scaled area of WSS < 0.4 Pa, the ratio of sinus diameter to ICA diameter and the scaled bifurcation angle for each case.

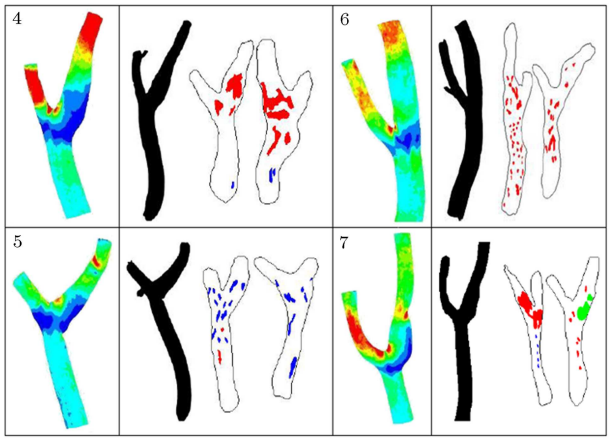

Figure 9. Comparison between the WSS contours and the results of pathomorphometrical analysis for geometry cases 4, 5, 6 and 7. The blue marks show fatty streaks and the red marks show fibrous plaques.

erated and cover a large area of blood vessels. This usually occurs at regions with critically low WSS. The area with low WSS is more discernable in geometries with greater ICA sinus diameter (geometry cases 4 and 7 shown in Figure 9).

CONCLUSION

In this study, we have investigated the steady Newtonian and non-Newtonian blood flow pattern in eight carotid bifurcation geometries. Three of these geometries are idealistic but close to reality; and five of them are reconstructed from patient specific data. The non Newtonian effect of blood has been investigated in these geometries. A factor has been represented to quantify the effect of a non-Newtonian blood model. The non-Newtonian behavior of blood is found to be atheroprotective. Unsteady flow has been solved in three idealistic geometries. The WSS of the sinus bulb was much lower than the total average WSS, as in steady solution. The WSS in the sinus bulb was found to be much less cyclic than the total WSS. An atherosclerosis risk factor has been defined based on the results of WSS. This risk factor agrees very well with the pathomorphometrical data of realistic bifurcations. The effect of bifurcation angle on WSS has been investigated in ideal geometries, but the results were not applicable to the realistic geometries because WSS is not related to the bifurcation angle in these cases. We have presented $D_{\text{sinus}}/D_{\text{ICA}}$ as a geometrical risk factor that agrees very well with the trend of the atherosclerosis risk factor.

ACKNOWLEDGMENTS

The authors gratefully acknowledge financial support (Grant # 87040150) from the Iran National Science Foundation (INSF). They are also grateful for the helpful comments of the anonymous referees.

REFERENCES

1. Tang, D., Yang, C., Mondal, S., Liu, F., Canton, G., Hatsukami, T.S. and Yuan, C. "Negative correlation between human carotid atherosclerotic plaque progression and plaque wall stress (low shear & disease)", *J. of Biomechanics*, **71**, pp. 727-736 (2008).
2. Malek, A.M., Alper, S.L. and Izumo, S. "Hemodynamic shear stress and its role in atherosclerosis", *J. of the American Medical Association*, **282**, pp. 2035-2042 (1999).
3. Oshinski, J.N., Curtin, J.L. and Loth, F. "Mean-average wall shear stress measurements in the common carotid artery (shear stress in common)", *J. of Cardiovascular Magnetic Resonance*, **8**, pp. 1-6 (2006).
4. Lee, S.W., Antiga, L., Spence, J.D. and Steinman, D.A. "Geometry of the carotid bifurcation predicts its exposure to disturbed flow", *Stroke*, **39**, pp. 2341-2347 (2008).
5. Younis, H.F., Kaazempur-Mofrad, M.R., Chan, R.C., Isasi, A.G., Hinton, D.P., Chau, A.H., Kim, L.A. and Kamm, R.D. "Hemodynamics and wall mechanics in human carotid bifurcation and its consequences for atherogenesis: investigation of inter individual variation", *Biomechanics and Modeling in Mechanobiology*, **3**(1), pp. 17-32 (2004).
6. Bressloff, N.W. "Parametric geometry exploration of the human carotid artery bifurcation", *J. of Biomechanics*, **40**, pp. 2483-2491 (2007).
7. Nguyen, K.T., Clark, C.D., Chancellor, T.J. and Papavassiliou, D.V. "Carotid geometry effects on blood flow and on risk for vascular disease", *J. of Biomechanics*, **41**(1), pp. 11-19 (2008).
8. Syo, D.D., Franjic, B.D., Lovricevic, I., Vukelic, M. and Palenkic, H. "Carotid bifurcation position and branching angle in patients with atherosclerotic carotid disease", *Collegium Antropologicum*, **29**, pp. 627-632 (2005).
9. Goubergrits, L., Affeld, K., Fernandez-Britto, J. and Falcon, L. "Investigation of geometry and atherosclerosis in the human carotid bifurcations", *J. of Mechanics in Medicine and Biology*, **3**(1), pp. 31-48 (1999).
10. Wells, D.R., Archie, J.P. and Kleinstreuer, C. "Effect of carotid artery geometry on magnitude and distribution of wall shear stress gradients", *J. of Vascular Surgery*, **23**, pp. 667-678 (1996).
11. Van Steenhoven, A.A., Van de Vosse, F.N., Rindt, C.C.M., Janssen, J.D. and Reneman, R.S. "Experimental and numerical analysis of carotid artery blood flow", *M. Atherosclerosis*, **15**, pp. 250-260 (1990).
12. Wootton, D.M. and Ku, D.N. "Fluid mechanics of vascular systems, diseases and thrombosis", *Annual Review of Biomedical Engineering*, **1**, pp. 299-329 (1999).

13. Gijsen, F.J.H., Van de Vosse, F.N. and Janssen, J.D. "The influence of the non-Newtonian properties of blood on the flow in large arteries: steady flow in a carotid bifurcation model", *J. of Biomechanics*, **32**(6), pp. 601-608 (1999).
14. Ding, Z., Wang, K., Lia, J. and Conga, X. "Flow field and oscillatory shear stress in a tuning-fork-shaped model of the average human carotid bifurcation", *J. of Biomechanics*, **34**(12), pp. 1555-1562 (2001).
15. Thomas, J.B., Antiga, L., Che, S.L., Milner, J.S., Hangan Steinman, D.A., Spence, J.D., Rutt, B.K. and Steinman, D.A. "Variation in the carotid bifurcation geometry of Young versus older adults", *Stroke*, **36**, pp. 2450-2456 (2005).
16. Carroll, T.J., Korosec, F.R., Petermann, G.M., Grist, T.M. and Turski, P.A. "Carotid bifurcation evaluation of time-resolved three-dimensional contrast-enhanced MR angiography", *Radiology*, **220**, pp. 525-532 (2001).
17. Zhao, S.Z., Ariff, B., Long, Q., Hughes, A.D., Thom, S.A., Stanton, A.V. and Xu, X.Y. "Inter-individual variations in wall shear stress and mechanical stress distributions at the carotid artery bifurcation of healthy humans", *J. of Biomechanics*, **35**, pp. 1367-1377 (2002).
18. Piersol, N.E., Lee, S., Kalata, W., Loth, F., Fischer, P.F., Leaf, G., Alperin, N. and Bassiouny, H.S. "Automated simulation of velocity and wall shear stress patterns inside a healthy carotid bifurcation", *2001 ASME Bioengineering Conference*, **50**, Snowbird, Utah, pp. 755-756 (2001).
19. Thomas, J.B., Che, S.L., Milner, J.S., Antiga, L., Rutt, B.K., Spence, J.D. and Steinman, D.A. "Geometric characterization of the normal and mildly diseased human carotid bifurcation", *2003 ASME Bioengineering Conference*, **1**, Sonesta Beach Resort in Key Biscayne, Florida, pp. 323-324 (2003).
20. Kaazempur-Mofrad, M.R., Younis, H.F., Patel, S., Isasi, A., Chung, C., Chan, R.C., Hinton, D.P., Lee, R.T. and Kamm, R.D. "Cyclic strain in human carotid bifurcation and its potential correlation to atherogenesis: Idealized and anatomically-realistic models", *J. of Engineering Mathematics*, **47**, pp. 299-314 (2003).
21. Zhao, S.Z., Xu, X.Y., Hughes, A.D., Thom, S.A., Stanton, A.V., Ariff, B. and Long, Q. "Blood flow and vessel mechanics in a physiologically realistic model of a human carotid arterial bifurcation", *J. of Biomechanics*, **33**, pp. 975-984 (2000).
22. Soulis, J.V., Giannoglou, G.D., Chatzizisis, Y.S., Seralidou, K.V., Parcharidis, G.E. and Louridas, G.E. "Non-Newtonian models for molecular viscosity and wall shear stress in a 3D reconstructed human left coronary artery", *Medical Engineering and Physics*, **30**, pp. 9-19 (2007).
23. Jahanifard, A., Firoozabadi, B. and Goodarzvand Chegini, A. "Computational simulation of non-Newtonian blood flow in carotid bifurcation for investigation the various rheological blood models", *Int. Mechanical Engineering Congress and Exposition*, Seattle, Washington, USA, pp. 1-8 (11-15 Nov. 2007).
24. Hyun, S., Kleinstreuer, C. and Archie, J.P. "Computational analysis of effects of external carotid artery flow and occlusion on adverse carotid bifurcation hemodynamics", *J. of Vascular Surgery*, **37**, pp. 1248-1254 (2003).
25. Urquiza, S., Blanco, P., Lombera, G., Venere, M. and Feijoo, R. "Blood flow finite element solution through the carotid artery", *Mecnica Computacional*, **22**, Baha Blanca, Argentina, pp. 232-243 (2003).
26. Marshall, I., Zhao, S., Papathanasopoulou, P., Hoskins, P. and Xu, X.Y. "MRI and CFD studies of pulsatile flow in healthy and stenosed carotid bifurcation models", *J. of Biomechanics*, **37**, pp. 679-687 (2004).
27. Blanco, P.J., Pivello, M.R., Feijóo, R.A. and Urquiza, S. "Sensitivity of blood flow at the carotid artery to the heart inflow boundary condition", *3rd Int. Congress on Computational Bioengineering*, Isla de Margarita, Venezuela (2007).
28. Bharadvaj, B.K., Mabon, R.F. and Giddens, D.P. "Steady flow in a model of the human carotid bifurcation. Part I: Flow visualization", *J. of Biomechanics*, **15**, pp. 349-362 (1982).
29. Bharadvaj, B.K., Mabon, R.F. and Giddens, D.P. "Steady flow in a model of the human carotid bifurcation. Part II: Laser-Doppler measurements", *J. of Biomechanics*, **15**, pp. 363-378 (1982).

BIOGRAPHIES

Seyedeh Samira Jamalian Ardakani after finishing high school studies in the fields of Mathematics and Physics in 2005, began her B.S. degree at Sharif University of Technology in the field of Mechanical Engineering. During her B.S. studies, she focused on Biomechanics related subjects; her thesis topic being "Modification of Lumped Parameters in Bifurcating Vessels". After graduation in 2010, she was awarded a direct PhD position at Texas A&M University in the Department of Biomedical Engineering. Her research is focused on the Effect of Mechanical Stimuli on Vascular Endothelial Cells.

Mohamad Jafarnejad after finishing his high school studies in the fields of Mathematics and Physics in 2005, began his B.S. degree at Sharif University of Technology in the field of Mechanical Engineering. During his B.S. studies, he focused on Biomechanics related subjects; his thesis topic being "Mechanical Simulation of a Cell Adhesion". After graduation in 2010, he was awarded a direct Ph.D. position at Texas A&M University in the Department of Biomedical Engineering. His research is focused on the Effect of Mechanical Stimuli on Vascular Endothelial Cells.

Bahar Firoozabadi is associate professor in the school of mechanical engineering at Sharif University

of Technology, Tehran. Her research interests are fluid mechanics in density currents, presently focusing on bio fluid mechanics, and porous media. She received her Ph.D. in mechanical engineering also at Sharif University. She teaches fluid mechanics and gas dynamics for undergraduates, and viscous flow, advanced fluid mechanics, continuum mechanics and biofluid mechanics for graduate students.

Mohammad Said Saidi is the professor of mechanical engineering at Sharif University of Technology. His research interests are: Modeling and Numerical Analysis of Transport and Deposition of Aerosol Particles, Modeling and Numerical Analysis of Biofluids, Modeling and Numerical Analysis of Thermal-Hydraulics of Porous Media and Microchannels.